Xerographic Response of an Aging Conductive Developer*

Robert J. Nash,[†] John T. Bickmore,[‡] W. H. Hollenbaugh, Jr.,[†] and Cheryl L. Wohaska
Xerox Corporation, 800 Phillips Road, Bldg. 139-65B, Webster, New York 14580

From a materials viewpoint, the xerographic developability of a conductive developer is governed by a balancing of opposing controlling parameters, namely toner concentration, toner triboelectric charge-to-mass ratio, and developer conductivity. For an age-induced decline in developer conductivity, the resultant decline in developability can be offset through an increase in toner concentration/decrease in toner charge-to-mass ratio. However, because an increasing toner concentration depresses developer conductivity, a critical loss in conductivity will trigger repeated increases in toner concentration and will hence provoke an accelerating trend to failure. In certain cases, however, a toner concentration–runaway failure can occur, even though the developer remains highly conductive, and for such cases the developability failure appears to be driven by physical factors such as the increased texture and reduced fluidity of a development brush having enhanced carrier-to-carrier contacts.

Journal of Imaging Science and Technology 40: 347–353 (1996)

Introduction

The conductive mode of development can provide a high rate of development[1–3] and a degree of development approaching full neutralization of an electrostatic latent image. For a conductive developer, therefore, functional xerographic performance will depend on maintenance of developer conductivity, in addition to the usual triboelectric properties of toner charge-to-mass ratio and concentration.[4] Since developers always show a degree of aging with use, the xerographic performance of a conductive developer will represent an overall response to age-induced changes in both conductivity properties and triboelectric charging properties, and the interplay of these controlling factors may produce a complex overall xerographic response to developer aging.

From a developer materials viewpoint, one obvious complication is the effect of the toner concentration on the intrinsic developer conductivity and triboelectric charging performance—for example, at any particular developer age, the developer conductivity will show an exponentially declining response to toner concentration,[4,5] and the developer triboelectric charge-to-mass ratio will show an inverse response to toner concentration.[6,7] Xerographically, these responses to toner concentration will produce opposing effects: the rate of xerographic development will decrease as developer conductivity decreases, but will increase as the toner charge-to-mass decreases.[1,3] These opposing influences clearly pose an interesting challenge for stable process control, especially if the toner concentration is used as the affected variable in a feedback control process having output image density as the target function. Additionally, age-induced changes in developer properties will be yet another further complication, especially since conductivity and triboelectric aging will generally occur at characteristically different rates.[5,8]

In the present report, the interplay between xerographic development and the intrinsic properties of an aging conductive developer is illustrated through a coupling of a simple descriptive model for conductive development with phenomenological descriptors for the aging of developer conductive and triboelectric properties. In particular, this approach is used to predict the set of xerographic material properties (i.e., toner charge-to-mass ratio, toner concentration, and developer conductivity) that provide a constant degree of image development as a developer ages, and the predictions are critically compared with actual experimental data from aging tests made on a range of conductive developers.

Theory

Developer aging can have a significant effect on the xerographic development of line images, solid-area images, and the background area. For this report, however, only solid-area image development will be considered. From published theoretical models and experimental studies,[1–3,9-16] solid-area xerographic development can be partitioned into several distinct limiting cases. These are:

(a) Initial Development/Insulative Magnetic Brush. In this case, successive development of toner particles from the development magnetic brush leaves an increasing level of counter-charge on the toner-depleted carrier beads, and this charge accumulation effectively collapses the development field, thus leaving the latent electrostatic image only partially neutralized by the developed toner particles. For a low level of development from an insulative magnetic development brush (i.e., for the case where toner supply is not a limiting factor), the mass of toner developed per unit area of image is given by:

$$m_{ins} \approx \varepsilon_0 v \cdot (V_D - V_{D0}) / (q/m \cdot l_{eff}), \qquad (1)$$

where ε_0 is the permittivity of free space; ν is the development roller/photoreceptor speed ratio; $V_D = (V_i - V_{BIAS})$ and V_i is the electrostatic latent image potential on the photoreceptor and V_{BIAS} is a dc bias applied to the development roller to suppress unwanted development of low image potential images; V_{D0} is an apparent development "offset" threshold potential below which development ceases; q/m is the average toner charge-to-mass ratio; and l_{eff} is the

Original manuscript received January 25, 1996. Revised May 20, 1996.

* Presented at IS&T 's 11th International Congress on Advances in Non-Impact Printing Technologies, October 29 – November 3, 1995, Hilton Head, SC.

† IS&T Member

‡ IS&T Fellow

dielectric thickness of the inactive region of the development magnetic brush, i.e., the region bounded by the carrier counter-charge.

(b) Initial Development/Conductive Magnetic Brush. At low levels of development with a conductive magnetic brush, the carrier counter-charge is dissipated by electrical conduction through the conductive carrier bead chains, and xerographic development can therefore proceed toward complete neutralization of the latent electrostatic image by developed toner particles. For such a case:

$$m_{cond} \approx \varepsilon_0 \cdot (V_D - V_{D0})/(q/m \cdot l_{pr}), \tag{2}$$

where l_{pr} is the effective dielectric thickness of the photoreceptor.

(c) Supply-Limited Development. For high levels of development, the available supply of toner from the magnetic brush becomes an important limiting factor. In particular, for a conductive magnetic brush, where the interior is essentially field-free, development will be limited by the amount of toner held at the exterior tips of the development brush. For this case:

$$m_{supply} \approx \rho_c \cdot PF \cdot h \cdot C \cdot v, \tag{3}$$

where ρ_c is the carrier mass density, PF is the carrier packing fraction, h is the depth of the "active" exterior layer of the development brush, and C is the weight percent of toner concentration.

(d) Overall Descriptor. For increasing levels of development potential, xerographic development will transition from an initial linear development mode to a final saturated (i.e., supply-limited) mode, and this transitional behavior (for both insulative and conductive development) can be approximated by a general connecting expression of the form:

$$m_{dev} \approx m_{supply} \cdot (1 - exp\{-m_{initial} / m_{supply}\}). \tag{4}$$

For low levels of development, a limiting generic descriptor can be written as:

$$m_{dev} \approx m_{initial} \approx \kappa \cdot (V_D - V_{D0})/(q/m), \tag{5}$$

where the proportionality constant κ is related to the dielectric properties of the development zone as detailed in Eqs. 1 and 2 for insulative and conductive development, respectively, and $\kappa_{cond} > \kappa_{ins}$.

For any particular toner, Eq. 5 can be further approximated, with developed mass replaced by developed image density:

$$SAD \approx \kappa^* \cdot (V_D - V_{D0})/(q/m), \tag{6}$$

where SAD is the reflection optical density of a developed solid-area image, and the proportionality constant κ^* incorporates the developed mass-to-image density transform. (For nonsaturated levels of optical density, the mass-to-image density relationship is closely linear, i.e., for any fixed toner size $\kappa^* \approx \kappa \cdot s$, with the scale factor s being a decreasing function of toner size, since optical covering power increases as toner size decreases).

Because the proportionality constant κ^* in Eq. 6 is directly related to κ_{cond} and κ_{ins}, Eq. 6 can be used as a concise descriptor for the relationship between image development and the important developer material properties of toner charge and developer conductivity. For example, since the experiments in this present report involve the xerographic response of conductive developers at a low development potential and a high level of toner concentration (i.e., conditions not constrained by toner supply), Eq. 6 can be used as a convenient conceptual framework for the analysis of the experimental data taken as the developers age toward an insulative state. Accordingly, this strategy will be outlined in the Results section of this report.

Experimental

Materials. *Carrier*. Atomized iron grit powder of nominal 130-μm diam, oxidized and lightly coated with about 0.1 wt% of polyvinylidene fluoride.

***Toner*.** Styrene/*n*-butyl methacrylate copolymer, melt-mixed with 6 wt% of a furnace carbon black, and with about 2 wt% of various positive charge control agents.[17] The toner was size-classified to a volume median diameter of about 11 μm.

***Developer*.** The carrier was preblended for 30 min. with toner at a concentration of 0.3 wt%, and then blended with toner at 2 wt% for 10 min. to produce the test developer.

Measurement Procedures. Toner charge and concentration were measured using a total blow-off of toner from developer held in a Faraday cage fitted with 36-μm steel-mesh screens. A miniature magnetic brush[4,5] was used to hold developer or detoned carrier samples against a 3-cm^2 guarded electrode, at a spacing of 2.54 mm. To minimize triboelectric charging current contributions, the conduction current was measured across a stationary brush at an applied potential of 10 V dc, i.e., at a voltage well below the highly non-ohmic "breakdown" level.

Aging Fixture. A toner throughput aging fixture was used to age the test developers at a constant output developed density. A dual-roller developer housing, containing 5400 g of developer, was set to operate in a single-roll mode with the upstream roller spaced 2.8 mm from a selenium alloy drum photoreceptor. The development roller-to-photoreceptor speed ratio was 2.09 in an "against" mode. With the photoreceptor surface potential kept discharged close to zero, image and background development was produced through a cyclic application of a dc potential of +75 and −75 V to the development roller. A target image density of 1.2 o.d. was generated during 6% of the imaging cycle, and an infrared density sensor was used to produce a feedback signal to the toner dispenser. The average toner consumption rate was about 100 g per hour.

At regular intervals, small samples of developer were removed for triboelectric and other physical measurements. Less frequently, 50 mL of developer were temporarily removed from the development roller for electrical conductivity measurements. For measurements on samples having a low level of conductivity, the test sample was incrementally detoned, and the sample conductivity was calculated by extrapolation of the detoned measurements.

Results

Test 1: Nominal Developer Conductivity. Beyond an initial transient increase in charging performance, the developer triboelectric properties of the test developer were very stable throughout 145 h of aging.

As discussed elsewhere,[6,7] the triboelectric response of a xerographic developer can be conveniently monitored through an A_t parameter, defined as:

$$A_t = q/m_t \cdot (C_t + C_0), \tag{7}$$

where q/m_t and C_t are the measured toner triboelectric charge-to-mass ratio and concentration values at any aging time t, and C_0 is a characteristic constant for any particular toner/carrier combination (e.g., C_0 is 1.0 for the present developers). As can be seen from Eq. 7, the A_t parameter directly mirrors changes in developer charging

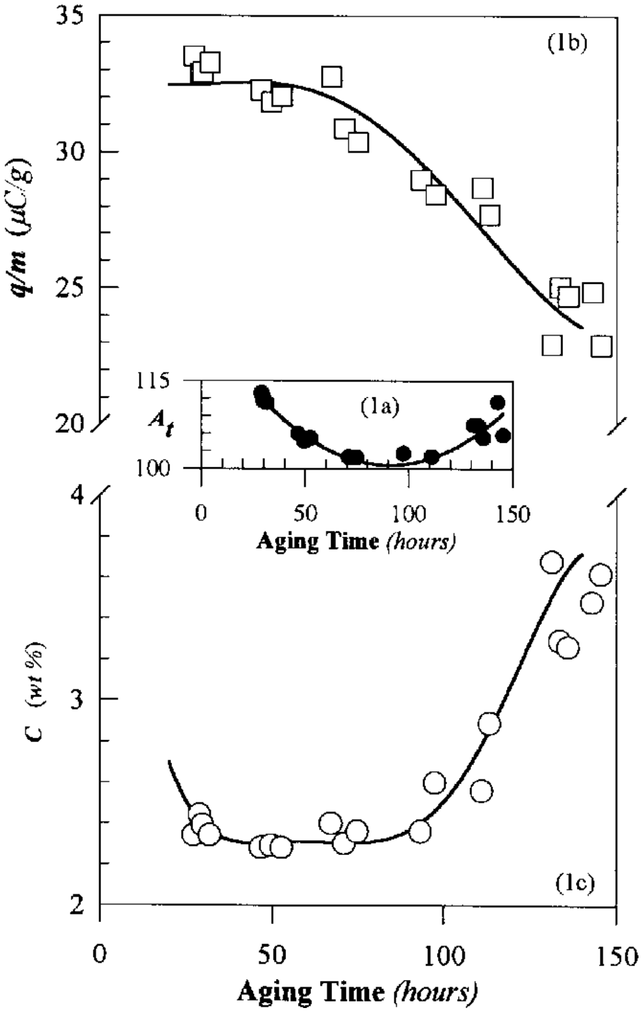

Figure 1. Experimental triboelectric aging data for Developer 1. [The lines in Figs. 1(b) and 1(c) are from a simulation; see text].

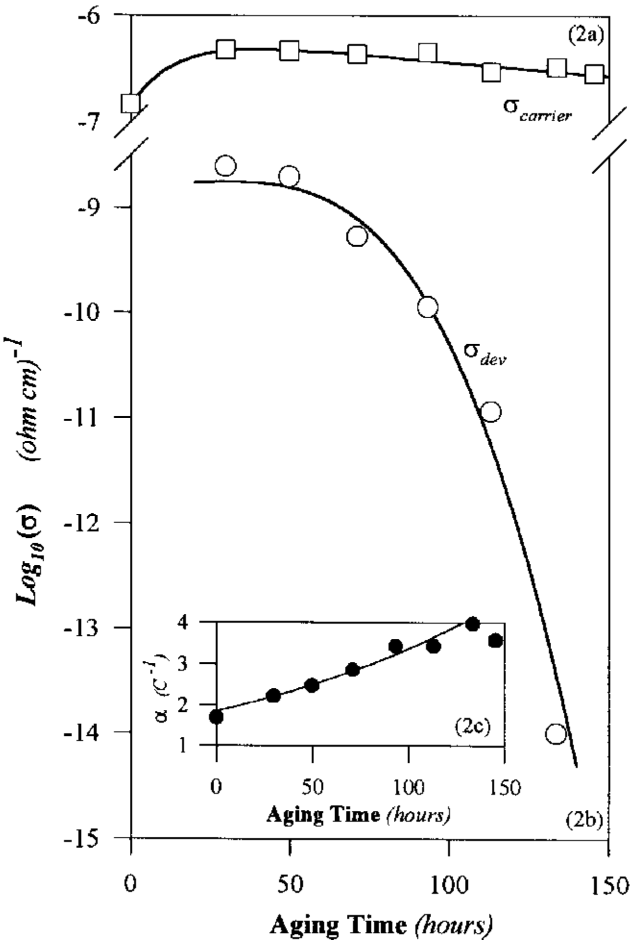

Figure 2. Experimental conductivity aging data for Developer 1. [The line in Fig. 2(b) is from a simulation; see text].

performance, and the A_t, aging time response, shown in Fig. 1(a) illustrates the level of charging stability of the developer in Test 1.

Whereas the A_t values in Fig. 1(a) varied only by ±5 around an average value of 105, Figs. 1(b) and 1(c) show that the corresponding q/m_t and C_t values varied quite widely and systematically during the aging test. Evidently, the xerographic developability of the test developer declined during the latter stages of the test, and, since the test developer was designed for the conductive mode of development, it is reasonable to suspect that the marked increase in C_t and decrease in q/m_t reflect an age-induced loss in developer conductivity. Figures 2(a) and 2(b) show the conductivity aging data from the detoned carrier and toned developer, respectively, and there is indeed a large decline in developer conductivity with age.

At any fixed developer age, developer conductivity can be related to carrier conductivity by:[4,5]

$$\sigma_{dev} = \sigma_{carrier} \cdot exp\{-\alpha \cdot C\}, \qquad (8)$$

and Figs. 2(a) and 2(c) show that the decline in developer conductivity seen in Test 1 is largely the result of an age-induced increase in the conductivity proportionality factor α.

The aging results from the developer studied in Test 1, then, can be viewed as an example of a xerographic response to developer conductivity aging coupled with stable triboelectric charging, and the experimental data can be used to define the form of the relationship between development and developer functional properties. However, because the aging data were taken at a single fixed output image density from a single fixed development potential, a further level of simplification must be applied to Eq. 6 before the analysis can be made. For example, developed solid-area density scans against applied development potential, made at occasional intervals throughout the aging test, were consistently linear with an extrapolated value of V_{D0} in the range of –25 ± 5 V. Consequently, $(SAD \cdot q/m)$, the product of the experimental solid-area density values and the corresponding q/m values should be approximately proportional to the κ^{*} parameter of Eq. 6, and a plot of $(SAD \cdot q/m)$ versus developer conductivity can therefore be used as a surrogate descriptor of the impact of developer conductivity on initial xerographic development.

Figure 3 shows the experimental $(SAD \cdot q/m)$ response to developer conductivity generated from the data taken during the developer aging process in Test 1 [high values of $(SAD \cdot q/m)$ are from the fresh conductive developer, and low values are from the eventual aged developer], and the plot indeed has the generally sigmoidal shape expected from models of xerographic development.

The data in Fig. 3 can be empirically described by

$$(SAD \cdot q/m) = 40.8 - [(40.8 - 27.8) \cdot exp\{-(\sigma_{dev} \cdot 7 \times 10^{9})^{0.28}\}], \qquad (9)$$

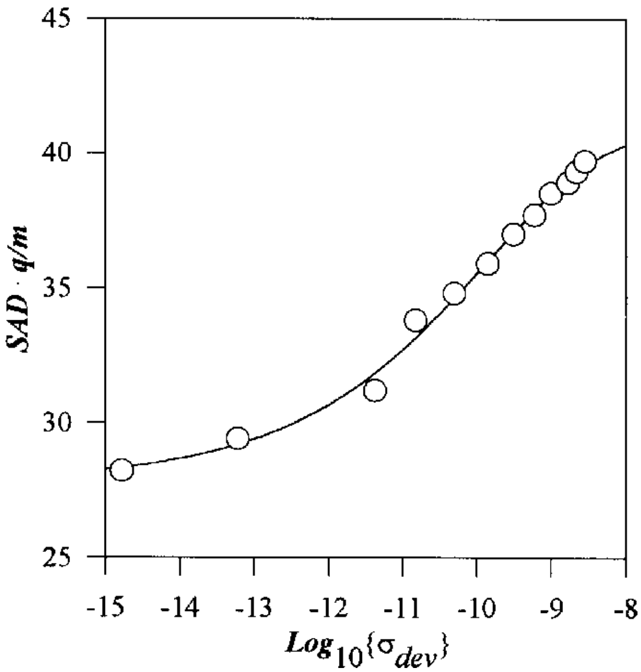

Figure 3. $(SAD \cdot q/m)$ versus $\log_{10}\{\sigma_{developer}\}$ for Developer 1. (Points are from individual smoothed plots of q/m versus age and $\log_{10}\{\sigma_{developer}\}$ versus age).

where 40.8 and 27.8 are the limiting $(SAD \cdot q/m)$ values for conductive and insulative development for the conditions of the present test.

The impact of developer aging on xerographic development can now be readily demonstrated, using Eq. 9 in conjunction with empirical descriptors for the triboelectric and conductivity aging responses. For convenience, the necessary calculations are most readily made using an iterative computer program to vary the toner concentration value until the calculated *SAD* value matches the target 1.2 o.d. value. In brief, the procedure is:

(a) Select an aging time, t
(b) Calculate A_t from polynomial fit:
$A_t = 125 - 0.544 \cdot t + 0.003 \cdot t^2$
(c) Select a low value of toner concentration, C
(d) Calculate q/m_t from:
$q/m_t = A_t / (C_t + 1)$
(e) Calculate carrier conductivity from:
$\sigma_{carrier} = 1.5 \,.\, 10^{-7} \cdot exp\,(1.5 \cdot (1 - exp\{-0.072 \cdot t\}))$
$\cdot\, (exp\{-0.006 \cdot t\})$
(f) Calculate α from:
$\alpha = 1.85 \cdot exp\{+0.006 \cdot t\}$
(g) Calculate developer conductivity from:
$\sigma_{dev} = \sigma_{carrier} \cdot exp\{-\,\alpha \cdot t\,\}$
(h) Calculate $(SAD \cdot q/m_t)$ from:
$(SAD \cdot q/m_t) =$
$40.8 - [(40.8 - 27.8) \cdot exp\{-(\sigma_{dev} \cdot 7 \times 10^9)^{0.28}\}]$
(i) Calculate *SAD* from:
$SAD = (SAD \cdot q/m_t) / (q/m_t)$
(j) If $SAD = 1.20 \pm 0.01$ then PRINT t, C_t, q/m_t, σ_{dev} ; increment t; return to (b)
(k) If $SAD < 1.20$, then increase C and return to (d)
(l) If $SAD > 1.20$, then decrease C to previous value; reduce the C increment and return to (d).

By varying the value of C until the target *SAD* value is achieved, the above computational scheme is a zero-order simulation of the behavior of a xerographic machine operating at a fixed-output image density via proportional control of the toner dispenser. Though based on a number of approximations, the overall simulation manages to capture the essential nonlinear aging tracks of the key developer functional parameters, i.e., toner concentration, toner charge and developer conductivity, and the solid lines in Figs. 1(b), 1(c), and 2(b) were generated from the computer simulation (continuous polynomial fits to simulation values calculated at interval of 10 h of aging).

Of course, the excellent fit between the calculated and experimental values shown in Figs. 1(b), 1(c), and 2(b) merely confirms the internal consistency of the computational scheme, since the experimental data were used to generate the fitting equations. However, the mechanics of the computational scheme provide a helpful illustration of the complex interplay between the controlling functional properties of an aging conductive developer. For example, as the rate of loss of developer conductivity increases, the decrease in q/m needed to maintain a constant output developed image density requires an increasing level of toner concentration, which in turn creates a further depression in developer conductivity. The net result, then, is a catastrophic, self-inflicted runaway failure, which, left unchecked, will drive the developer to a totally insulative mode of development.

The relationship shown in Fig. 3 represents a single-valued description of the xerographic response of an aging conductive developer for the specific process conditions used in the present aging tests, and it should be valid for any combination of developer conductivity and toner triboelectric charge. However, in reality, key material properties cannot be manipulated independently—for example, high toner charge-to-mass ratio/low developer conductivity can be achieved only with an aged developer, and low toner charge-to-mass ratio/high developer conductivity can be achieved only with a new conductive developer. Indeed, as can be seen from Eqs. 7 and 8, there will be a specific linear relationship between the logarithm of the developer conductivity and the inverse of the toner charge-to-mass ratio for each developer age,[2] with toner concentration being the controlling link between these two parameters. For example, if C is eliminated between Eqs. 7 and 8, then:

$$m/q_t = log_e\{\sigma_{dev}\} \cdot (-1/(A_t \cdot \alpha)) + (1/(A_t \cdot \alpha)) \cdot (log_e\{\sigma_{carrier}\}) + C_0/A_t, \tag{10}$$

so that a plot of m/q against $\log_e(\sigma_{dev})$ for any fixed developer age will have an extrapolated intercept of $(1/(A \cdot \alpha)) \cdot (\log_e\{\sigma_{carrier}\}) + C_0/A$ and a negative slope of $1/(A \cdot \alpha)$. Lines of constant output developed density (in the range of 1.2 o.d, and below) can also be readily drawn on an m/q: $\log_e\{\sigma_{dev}\}$ plane using the relationship given in Eq. 9. Figure 4 shows this type of mapping calculated for selected ages of the developer examined in Test 1. In this figure, each straight line represents a toner concentration scan at the noted developer age, and the nonlinear isodensity contours connect points of equal output image density for all possible developer ages. (Figure 4, of course, must be viewed as a design-space map rather than as a cause/effect graph for m/q and $\log\{\sigma_{dev}\}$.)

Now, if Eq. 9 is truly an accurate descriptor for the relationship between xerographic development and the functional materials properties of a developer when operated in the present aging fixture, then a critical test of the equation would be the prediction of the performance of a range

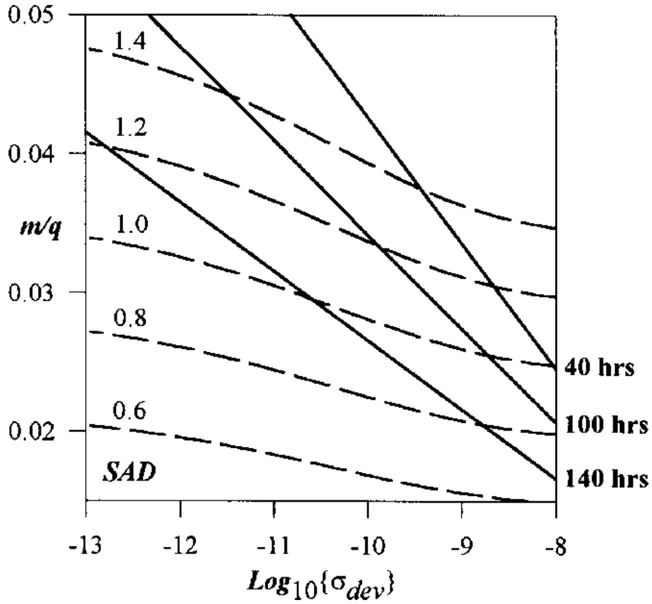

Figure 4. Predicted output isodensity contours for Developer 1. (For any developer age, a toner concentration scan will generate a specific linear m/q:$\log_{10}$ $\{\sigma_{developer}\}$ relationship. Only points on this line will be accessible.)

of developers in the fixture. As an example, the equation will next be used to predict the xerographic performance of two developers having material properties distinctly different than those of the developer used in Test 1.

Test 2: Reduced Developer Conductivity. For this test, the developer had an enhanced triboelectric value and somewhat depressed conductivity properties. As in Test 1, beyond an initial transient increase in charging performance, the developer triboelectric properties of this test developer, as shown in Fig. 5(a), were very stable throughout the aging test. However, once again, the stability indicated in the A_t:t plot conceals major compensatory changes in q/m_t and C_t, as shown in Figs. 5(b) and 5(c), and these plots reflect a xerographic system response to a major age-induced decline in developability. Figures 6(a), 6(b), and 6(c), which show the corresponding experimental conductivity data, clearly indicate a rapid decline in developer conductivity, driven by an increase in the α parameter with increasing aging time and by an increased operational toner concentration (a consequence of the higher value of A_t of this second test developer).

For the developer used in Test 2, the key descriptors of the aging performance of the functional materials properties are

$$A_t = 161 - 0.968 \cdot t + 0.008 \cdot t^2, \tag{11}$$

$$\sigma_{carrier} = 1.3 \cdot 10^{-7} \cdot exp(1.65 \cdot (1 - exp\{-0.15 \cdot t\}) \cdot (exp\{-0.013 \cdot t\}), \tag{12}$$

$$\alpha = 1.8 \cdot exp\{+ 0.013 \cdot t\}, \tag{13}$$

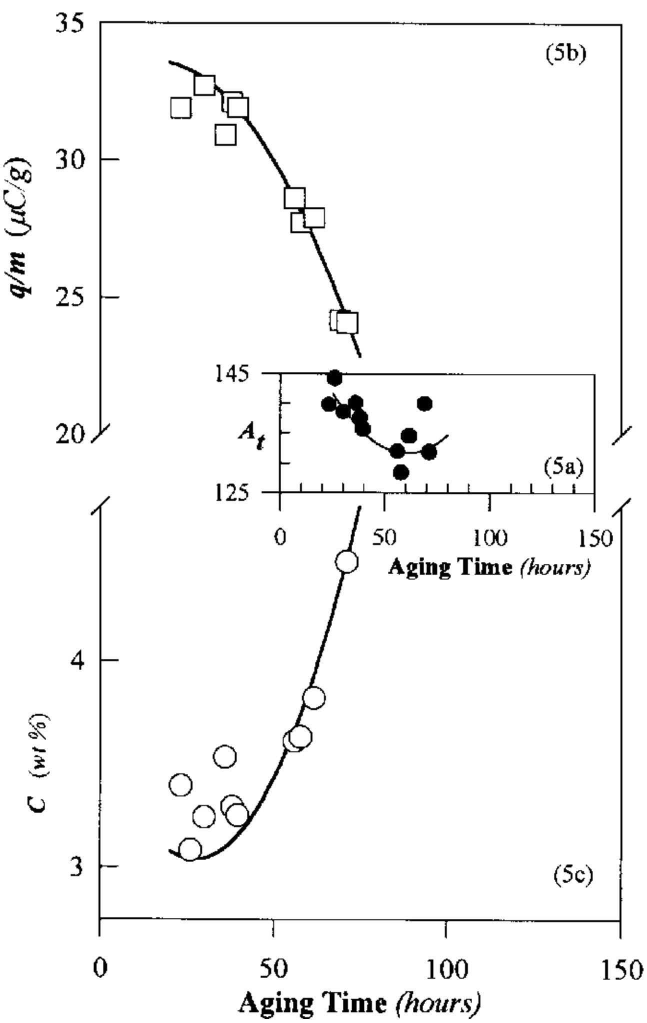

Figure 5. Experimental triboelectric aging data for Developer 2. [The lines in Figs. 5(b) and 5(c) are from a simulation; see text].

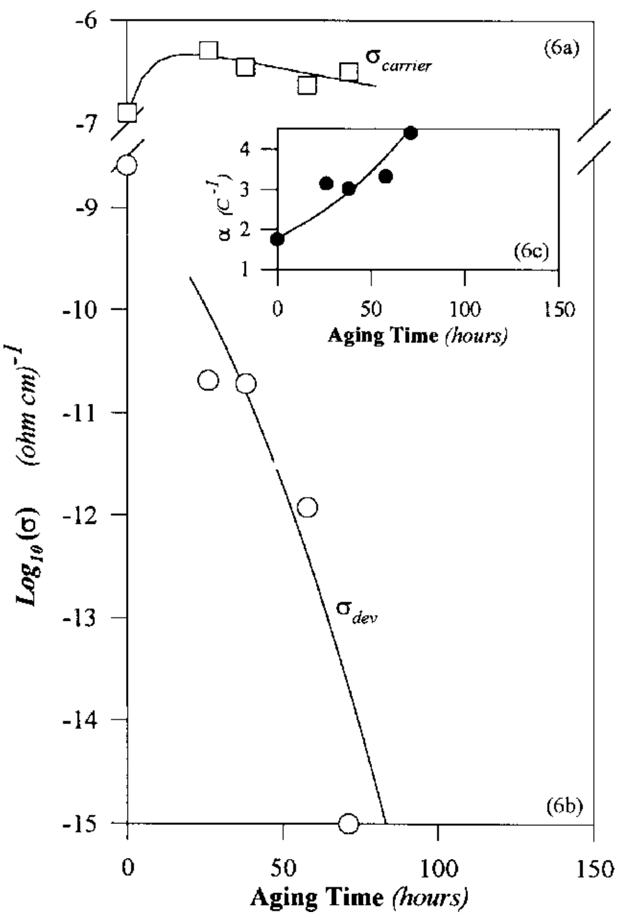

Figure 6. Experimental conductivity aging data for Developer 2. [The line in Fig. 6(b) is from a simulation; see text.]

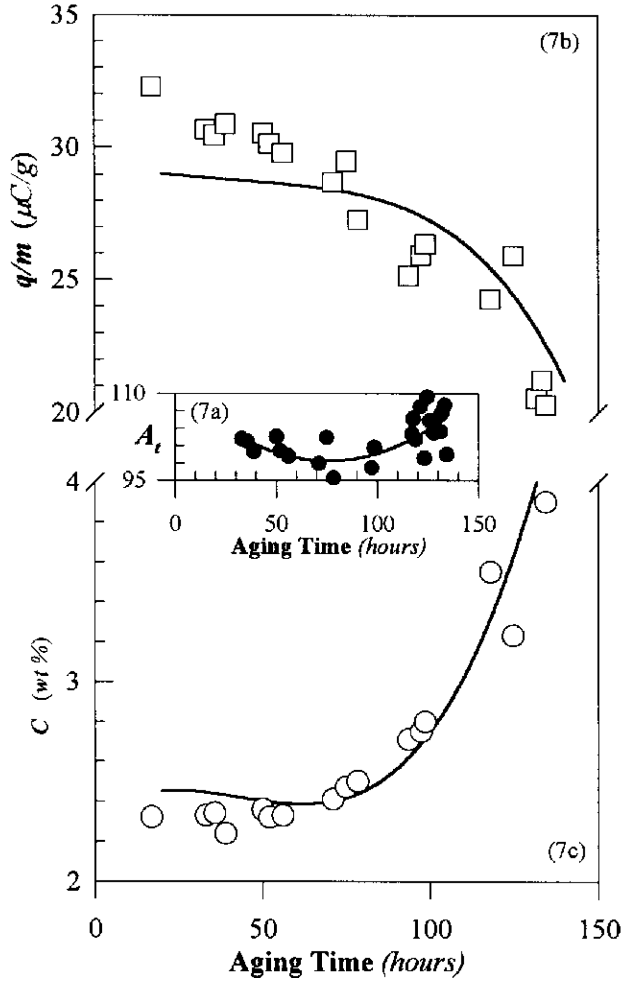

Figure 7. Experimental triboelectric aging data for Developer 3. [The lines in Figs. 7(b) and 7(c) are from a simulation; see text.]

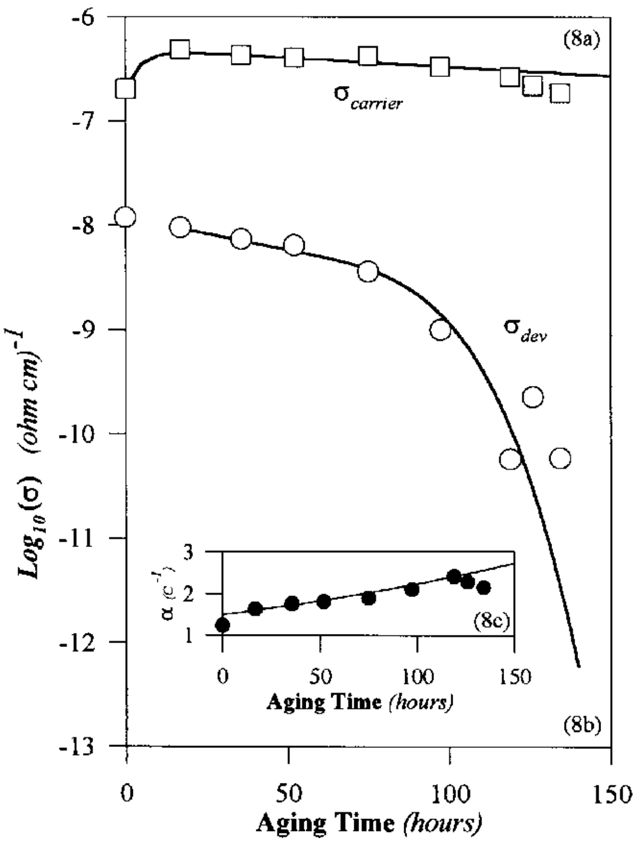

Figure 8. Experimental conductivity aging data for Developer 3. [The line in Fig. 8(b) is from a simulation; see text.]

and these equations, along with Eq. 9, deduced from Test 1, can broadly reproduce the observed rapid decline in xerographic developability. However, to predict the close match indicated by the solid lines in Figs. 5(b), 5(c), and 6(b), it was necessary to scale the ($SAD \cdot q/m$) values from Eq. 9 by a factor of 1.14. Possible reasons for this apparent enhanced developability will be considered in the final Discussion section of this report.

Test 3: Increased Developer Conductivity. For this test, the developer was triboelectrically similar to the developer in Test 1 and had superior conductivity stability. As in Test 1, beyond an initial transient increase in charging performance, the developer triboelectric properties of this test developer, as shown in Fig. 7(a), were very stable throughout the aging test. Once again, however, the stability indicated in the A_t:t plot conceals major compensatory changes in q/m_t and C_t, as shown in Figs. 7(b) and 7(c), and these plots reflect a xerographic system response to a major age-induced decline in developability. However, Figs. 8(a), 8(b), and 8(c), which present the corresponding experimental conductivity data, do not show any significant decline in conductivity parameters, and the experimental α values are noticeably low.

For the developer used in Test 3, the key descriptors of the aging performance of the functional materials properties are:

$$A_t = 111 - 0.335 \cdot t + 0.002 \cdot t^2, \quad (14)$$

$$\sigma_{carrier} = 2.0 \cdot 10^{-7} \cdot exp(0.90 \cdot (1 - exp\{-0.20 \cdot t\}) \cdot (exp\{-0.004 \cdot t\}), \quad (15)$$

$$\alpha = 1.5 \cdot exp\{+ 0.004 \cdot t\}, \quad (16)$$

and these equations, along with Eq. 9 deduced from Test 1, can broadly reproduce the observed eventual rapid decline in xerographic developability. However, to predict the close match indicated by the solid lines in Figs. 7(b), 7(c), and 8(b), it was necessary to scale the (SAD · q/m) values from Eq. 9 by a factor of 0.85. Possible reasons for this apparent diminished developability will be reviewed in the following Discussion section.

Discussion

The analysis of the experimental data from Tests 1, 2, and 3 indicate that the general developability relationship shown in Eq. 6 must be modified by the addition of a linear scaling factor, e.g.,

$$(\mathrm{SAD} \cdot q/m\,) \approx \kappa^{*} \cdot (\mathrm{V}_D - \mathrm{V}_{D0}) \cdot f\,, \quad (17)$$

where $f = 1$ for Test 1, $f = 1.14$ for Test 2 and $f = 0.85$ for Test 3. Of course, the variability in the scaling factor f must be accounted for if Eq. 17 is to have any predictive utility, and it will be convenient to separate the potential causes into extrinsic and intrinsic categories.

Extrinsic Causes. In the analysis thus far, the effective development potential, $(V_D - V_{D0})$, has been implicitly assumed to be constant. However, variability in V_{D0}, the "self-generated/internal bias," would act as an effective linear scaling factor for Eq. 6; for an applied imaging bias of +75 V and an average V_{D0} value of –25

V, the net effect on f of a fractional variability in V_{D0} of f^* would be

$$f = 0.75 + 0.25 \cdot f^{*}. \tag{18}$$

Because the observed variability in V_{D0} was ± 5 V, a variability in V_{D0} might account for only a 5% variability in the factor f. Also, *SAD*-development voltage scans taken on development-deficient developers showed that the loss in developability was a reflection of a decrease in the slope of the linear *SAD*-applied voltage relationship, rather than the result of any significant change in the extrapolated zero-development intercept value.

Accordingly, other factors that can affect the proportionality factor κ^* must be considered, and these effects include the conventional mechanical parameters that govern the supply of developer to the development nip—e.g., the developer-roller-to-photoreceptor spacing, the gap set by the magnetic brush trimming device, the various process speeds, the strength and orientation of the development roller magnet(s), and even the amount of developer present in the housing. Through variability in initial machine setup, these factors can cause differences from test to test, and in-run changes in settings can produce discontinuous changes in performance within a single test. Repeated tests on a single test developer show a level of test-to-test variability similar to that seen between Tests 1, 2, and 3, suggesting that extrinsic factors can be an important source of test variability. However, because the functional properties of developer materials can also be altered during use, extrinsic effects may not be the sole source of variability, even for tests on a single developer.

Intrinsic Causes. Because Eq. 6 involves the optical density of the developed solid area image, the covering power of the test toners must be considered as a potential source of test-to-test variability. However, the toners in Tests 1, 2, and 3 were all based on a single binder resin and a single carbon black, so they were equally opaque.

Toner size can affect developability in several ways, and a decrease in toner size would tend to produce an increase in the f factor. For example, starting from a nominal condition, a decrease in toner size increases *SAD*, increases α and, hence, decreases σ_{dev}, and (at low values of C) increases q/m. All of these changes create a positive offset to the $(SAD \cdot q/m)$:$log\,\{\sigma_{dev}\}$ relationship and hence lead to an $f > 1$ condition. For the toners in Tests 1, 2, and 3, however, there were no significant differences in toner size.

Whereas the data from Tests 2 and 3 can be adequately described using fixed values of a scaling factor applied to the developability relationship from Test 1, a close examination of the data indicates that the scaling factor actually declines linearly with aging time. Thus the scaling factor $f = 0.85$ applied to the data from Test 3 is actually an average of an initial value of 0.9 and a long-term value of 0.8. It would appear, then, that an additional age-induced component to the developability loss phenomenon occurs, and from tests made on a large series of model toners it appears that tests leading to $f < 1$ are associated with developers having a high and stable level of conductivity, and an impaired level of developer flow. The former observation seems counter-intuitive, since the conductive mode of development is more efficient than the insulative mode. However, taken together, the observations point to an indirect material-driven mechanism for developability loss. For example, since developer conductivity decreases with increasing toner concentration, a high level of conductivity (especially if maintained over a range of toner concentrations, i.e., if the α factor is low) implies a high carrier packing density.[4] For such a case, developer flow through metering/trimming regions in the development housing may be impaired, and the texture and form of the development brush may be inferior to that given by an optimum free-flowing developer. The net result will be an effective reduction in the value of the κ^* parameter, driven by a physical limitation in the supply of developer to the development nip. Such a mechanism might also explain the tendency for the factor f to decrease with aging time since the resultant increase in set-point toner concentration probably also adds to the reduction in developer fluidity.

Conclusions

In retrospect, it appears likely that the somewhat anomalous results from the present tests are a direct result of operation of the aging fixture in a mode of limited latitude (e.g., development from a single roller at a low imaging potential and a high operational toner concentration). If operated in a wide-latitude xerographic marking subsystem, the xerographic performance of the developers examined in Tests 1, 2, and 3 would be expected to show a reduced sensitivity to age-induced changes in the functional properties of the developers. Indeed, when tested in a dual-roller development housing in a commercial 90 prints/min. xerographic copier, developers of the type examined in Tests 1, 2, and 3 gave stable development throughout a 500K copy print evaluation.[17] In these actual imaging tests, the toner concentration remained stable at about 2 wt%, and there was no tendency toward an increase in toner concentration, even during the latter stages of the evaluation.

With respect to development subsystem robustness, it should also be noted that potential housing/developer interactions are only finally minimized during system optimization testing, since at that phase of product development the critical mechanical tolerances of a developer housing are optimized around the properties of a mature design-intent developer. For the present study, Test 1 represents the case of a matched developer material/development housing combination, and Tests 2 and 3 represent extreme examples (because of the severely constrained development latitude) of the potential xerographic impact of developer design modifications implemented without reoptimization of the development subsystem.

References

1. J. A. Benda and W. J. Wnek, *IEEE Trans Ind. Appl.* **1A-17**: 610–618 (1981).
2. W. J. Wnek, *Paper Summaries, SPSE's 42nd Ann. Conf.* 187–192 (1989).
3. L. B. Schein, G. Beardsley, and M. Moore, *J. Imaging Technol.* **16**: 129–135 (1990).
4. R. J. Nash, *Proceedings of SPSE's 5th International Congress on Advances in Non-Impact Printing Technologies,* J. Moore, Ed., 1989, pp. 158–165.
5. R. J. Nash and J. T. Bickmore, *Proceedings of IS&T's 8th International Congress on Advances in Non-Impact Printing Technologies* E. Hanson, Ed., 1992, pp. 131–139.
6. E. J. Gutman and G. C. Hartmann, *J. Imaging Sci. Technol.* **36**: 335-349 (1992).
7. R. J. Nash, S. M. Silence and R. N. Muller, *Proceedings of IS&T's 10th International Congress on Advances in Non-Impact Printing Technologies,* A. Melnyk, Ed., 1994, pp. 95–107.
8. R. J. Nash and J. T. Bickmore, *Proceedings of IS&T's 9th International Congress Advances in Non-Impact Printing Technologies* M. Yokohama, Ed. 1993 pp. 68–71.
9. W. S. Jewett, *Conf. Rec. 12th. Ann. Meeting IEEE-IAS* 557-568 (1977).
10. D. A. Hays, *J. Imaging Technol.* **15**: 29–38 (1989).
11. J. J. Folkins, *Conf. Rec. IEEE-IAS Ann. Meeting*, 1510–1514 (1985).
12. M. H. Lee and G. Beardsley, *J. Imaging Technol.* **13**: 29–37 (1987).
13. L. B. Schein, K. J. Fowler, G. Marshall and V. Ting, *J. Imaging Technol.* **13**: 60–67 (1987).
14. D. A. Hays, *IEEE Trans. on Ind. Appl.* **1A-23**, 970-974 (1987).
15. J. J. Folkins, *Proceedings of IS&T's 6th International Congress on Advances in Non-Impact Printing Technologies,* R. J. Nash, Ed., 1990, pp. 15–24.
16. G. P. Gee, *Proceedings of IS&T's 8th International Congress on Advances in Non-Impact Printing Technologies,* E. Hanson, Ed., 1992 pp. 46–50.
17. US Patent 5,304,449.